AIAA SciTech Forum
5-9 January 2015, Kissimmee, Florida
53rd AIAA Aerospace Sciences Meeting

10.2514/6.2015-1482

Gas-Phase Temperature Measurements in the Exhaust of a J85 Engine Using Coherent Anti-Stokes Raman Scattering

Andrew Alexander[1] and Joseph Wehrmeyer[2]
Aerospace Testing Alliance (ATA), Arnold AFB, TN 37389

Jason M. Kriesel[3]
Opto-Knowledge Systems, Inc. (OKSI), Torrance, CA 90502

Paul S. Hsu[4] and Sukesh Roy[5]
Spectral Energies, LLC, Dayton, OH 45431

and

Joseph D. Miller[6] and James R. Gord[7]
Air Force Research Laboratory, Wright-Patterson AFB, OH 45433

Coherent anti-Stokes Raman scattering (CARS) spectroscopy-based thermometry techniques have been developed to acquire spatially and temporally resolved measurements in laboratory flames. However, implementation of CARS techniques in practical combustion environments, such as gas-turbine-engine test facilities, is challenging. In addition to limited optical access, harsh environments associated with test facility applications (i.e., uncontrolled humidity, vibration, and large thermal gradients) often restrict the operation of high-power laser systems and the free-standing optics required for CARS measurements. Two CARS diagnostic systems were developed to mitigate issues encountered for acquiring CARS spectra and derived temperatures in harsh test cell environments. One is a nanosecond (ns) CARS system using fiber-coupled lasers, and the other is a transportable picosecond (ps) laser-based CARS system integrated within an environmental protection unit (EPU). In this effort fiber-coupled ns-CARS and direct-beam ps-CARS systems are implemented for gas-phase thermometry within the exit plane exhaust of a J85 turbine engine. Improvements of measurement sensitivity and accuracy are demonstrated by suppression of the nonresonant-background (NRB) signal utilizing a ps-probe-pulse-delay technique. The effects of environmental noise (e.g., vibration) are investigated.

Nomenclature

AB	=	afterburner
CARS	=	coherent anti-Stokes Raman scattering
CCD	=	charged-coupled device
FWHM	=	full-width at half-maximum
HCWG	=	hollow-core waveguide
MSIF	=	multimode step-index fiber
NA	=	numerical aperture

[1] Engineer, Aerospace Testing Alliance (ATA), andrew.alexander.1.ctr@us.af.mil
[2] Senior Engineer, Aerospace Testing Alliance (ATA), joseph.wehrmeyer.ctr@us.af.mil AIAA Senior Member
[3] Lead Scientist, Opto-Knowledge Systems Inc, Jason@oksi.com
[4] Research Scientist, Spectral Energies LLC, paul.hsu.ctr@us.af.mil AIAA Member
[5] Senior Research Engineer, Spectral Energies LLC, roy.sukesh@gmail.com, AIAA Associate Fellow
[6] Research Engineer, AFRL Aerospace Systems Directorate, joseph.miller.35@us.af.mil AIAA Senior Member
[7] Principal Research Chemist, AFRL Aerospace Systems Directorate, james.gord@us.af.mil, AIAA Associate Fellow

NRB = nonresonant background
PLA = power lever angle
SNR = signal-to-noise ratio

I. Introduction

COHERENT anti-Stokes Raman scattering (CARS) spectroscopy is a nonintrusive laser-based measurement technique that has been widely used for temperature and species-concentration measurements in reacting flows. [1,2] This technique can provide high-resolution spatial and temporal measurements. The CARS diagnostic technique is based on a 3rd-order nonlinear process involving precise spatial and temporal overlapping of three laser beams (pump, probe, and Stokes) positioned within the probe volume to generate a CARS signal. In air breathing combustion environments CARS measurements can be utilized to derive temperatures utilizing high concentrations of nitrogen molecules present throughout the combustion region. Traditional gas-phase CARS thermometric measurements were acquired using nanosecond (ns) laser pulses. An inherent challenge with this technique results from undesired contributions of the nonresonant background (NRB) signal[1-4] limiting the applicability, sensitivity, and accuracy of nanosecond CARS at higher pressures. This is especially prevalent in hydrocarbon-rich environments due to high nonresonant susceptibility of hydrocarbon compounds. The contribution of the NRB signal is highest when the pump and probe beams are overlapped temporally. Within the past decade, this encompassing issue has been resolved through the use of ultrashort pulses, specifically picosecond (ps) and femtosecond (fs) pulse durations. In the ps and fs regimes, it is possible to delay the probe beam temporally with respect to the pump beam to suppress the nonresonant contributions.[2] Additionally, with ultrashort pulses the real-time collisional lifetime of various molecular species can be measured using time-resolved ps-, fs-, and ps/fs-hybrid CARS.[5-8] The extracted collisional-lifetime information can be directly converted to the spectral widths of the individual Raman transitions of the target molecule. This conversion provides useful information to the CARS model, allowing more accurate and precise determination of temperature and species-concentrations.[2,5-8] Recently, fs- and ps/fs-CARS approaches were successfully demonstrated to allow collisional-free temperature determinations.[2,9,10]

Although many successful demonstrations have been performed in the laboratory, transitioning the CARS diagnostic systems for use in harsh environments, specifically turbine engine ground-test facilities, is especially challenging. Use of state-of-the-art CARS diagnostic systems in ground-test facilities relies on free-standing optics which must overcome challenges including limited optical access, vibrations, and the ambient air temperatures and humidity levels in test facility environments. Temperature and chemical species concentration measurements have been successfully demonstrated in test cell environments using the traditional ns-CARS approach. These environments include scramjet combustors,[11] hypersonic wind tunnels,[12] and rocket test stands.[13] However, to our knowledge, the recently developed ultrashort-pulse CARS techniques (i.e., ps-CARS, fs-CARS, ps/fs-CARS), which require better stabilization of the laser systems and optical alignment, as compared to ns CARS, have only been demonstrated in laboratory flame studies.

To resolve challenges associated with harsh test cell environments, several fiber-coupled CARS techniques have been recently developed for gas-phase thermometry applications. Hsu et al., demonstrated fiber-coupled ps-CARS thermometry using multimode step-index fibers (MSIFs).[14,15] Due to their high optical-damage threshold low transmission and bending losses, MSIFs are ideal for practical applications requiring transmission of high-power laser beams. However, these systems are hampered by non-negligible spectral broadening of the CARS beams, depolarization of the delivered beams, and poor beam quality at the output of the fiber. These problems significantly degrade the CARS spectral resolution and signal-to-noise ratio (SNR), especially at longer fiber lengths (> 3 m).[15] A possible solution to these issues is the use of specially designed, air-guided, hollow-core waveguides (HCWGs). HCWGs offer the potential for delivering laser pulses of sufficient energy over long distances with low nonlinearity. The use of HCWGs may enable gas-phase thermometry using CARS spectroscopy.[16] Because guiding is accomplished via Fresnel reflection, these fibers are more susceptible to energy loss than MSIFs. Kriesel et al., investigated the use of high-power laser-beam delivery through HCWGs for CARS applications. This research demonstrated the ability of HCWGs to deliver the energy levels required for ns-CARS applications with small-radius fiber bending.[16]

This paper reports results of fiber-coupled and direct-beam CARS techniques for N_2 thermometry applied within the near-field exhaust of a J85 turbine engine**.** In this effort fiber-coupled ns-CARS and direct-beam ps-CARS systems were implemented for gas-phase thermometry within the exit plane exhaust of a J85 turbine engine. An environmental protection unit (EPU) was designed, fabricated, and demonstrated for acquiring ps-CARS measurements in harsh environments associated with turbine engine ground-test facilities. For direct-beam ps-CARS

measurements, ps vibrational CARS (ps-VCARS) with a BOXCAR geometry and ps rotational CARS (ps-RCARS) with crossed two-beam geometry were demonstrated. In addition, suppression of the nonresonant background (NRB) signal using the ps-probe-pulse-delay technique and the effects of environmental noise (e.g., vibration) were investigated.

II. Propulsion Research Facility (PRF): J85-GE-5 Engine

The instrumentation and diagnostics team at the Arnold Engineering and Development Complex (AEDC) is responsible for the development and application of innovative diagnostic techniques and analysis tools to address AEDC test customer requirements. Diagnostic systems are routinely evaluated in a test bed facility at the Propulsion Research Facility (PRF) located on the campus of the University of Tennessee Space Institute (UTSI) adjacent to AEDC. This test bed is jointly operated by AEDC and UTSI personnel. The test bed is utilized to advance the Technology Readiness Level (TRL) by providing a realistic test environment to demonstrate diagnostic systems and reduce the risk of utilizing diagnostic systems inside test facilities. For these demonstration tests, a J85-GE-5 turbine engine was operated in the PRF as a test asset to provide high-enthalpy flow conditions for evaluating the CARS systems. The J85-GE-5 engine is a high-thrust, lightweight turbojet engine currently used in several aerospace propulsion applications, most notably the USAF T-38 Talon aircraft. It has an eight-stage, high-lift, axial-flow compressor driven by a two-stage turbine rotor. The engine incorporates a through-flow, annular-type combustion system, controlled compressor interstage bleed air, and an afterburner (AB) with a variable-area exit nozzle. The basic afterburner can section is ~ 280 cm in length and 50 cm in diameter. Engine dry mass with AB is 265 kg (584 lbm). The engine thrust at standard day, sea-level-static conditions is 2,680 lbf at military power and 3,850 lbf at maximum AB operation. Nozzle-exit, exhaust-gas temperatures range from 480ºC (900ºF) at idle to 1,760ºC (3,200ºF) at maximum afterburning conditions.[17] Figure 1 shows the J85 engine installed and operating in the PRF facility for evaluation of probe hardware. The probes in Figure 1 are not related to this work. The diagnostic probes are shown inserted in the exhaust flow immediately downstream of the nozzle exit plane.

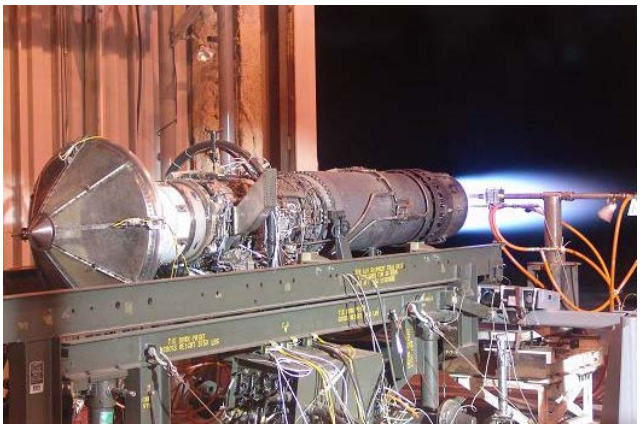

Figure 1. GE-J85-5 engine mounted on an A/M37-T20 thrust stand in the PRF facility.

III. Evaluation of the HCWG ns-CARS at the PRF

The HCWG ns-CARS system employs a portion of the Spectra-Physics frequency-doubled Nd:YAG (532-nm) output from a Spectra Physics Quanta Ray, Model Pro 290 to pump a modeless dye laser (built by Spectral Energies, LLC) to generate broadband pulses at ~607 nm for N_2 CARS applications. The pulse width of the 532-nm and 607-nm beams is ~8 ns. These two beams (~18 mJ at 532 nm and ~10 mJ at 607 nm) are focused into separate 5-m-long, 750-μm HCWGs. The pulse energy required for ns-CARS is much higher than that required for ultrafast CARS.[14] HCWGs have a much higher damage threshold than solid-core MSIFs, making them more suitable for ns-CARS applications. Figure 2a shows a schematic of fiber structure. The HCWGs are fabricated by flowing a silver solution through a glass capillary tube, as illustrated in Fig. 2b. Note that for HCWGs intended for infrared wavelengths, an additional dielectric layer is deposited on top of the silver layer. For visible wavelengths, such as those used in this experiment, the silver is not coated. For acceptable transmission in the visible-wavelength range, the silver surface must be extremely smooth. Two HCWGs manufactured by Opti-Knowledge Systems Inc, or OKSI were used throughout the engine tests. The HCWGs performed as expected and did not degrade throughout the tests.

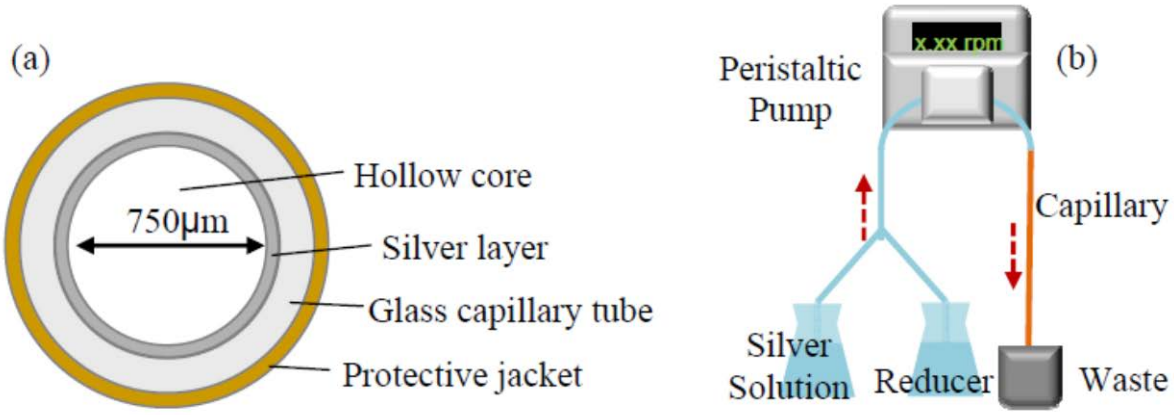

Figure 2. (a) Diagram of a silver-coated HCWG and (b) simplified schematic illustrating the method for applying silver coating to the inside of a glass capillary tube.

To achieve high laser-to-fiber-coupling efficiency and better output-beam quality (M^2), the input laser beams were coupled into the fiber with a small numerical aperture (NA ~0.01). This was attempted initially with the use of long-focal-length lenses (f = 750 mm or f = 1,000 mm), which resulted in increasing the spot size at the focal point. The larger spot size also decreases the risk for dissociation of air in front of the HCWG. This effectively enables the use of higher energy beams. Other nuances associated with longer focal lengths include 1) the additional space required on the optical table; 2) the possibility that the focused spot is larger than the fiber-bore diameter; and 3) the possibility that if the beam quality is poor, a long-focal-length lens may not focus the spot size smaller than the bore of the HCWG. Generally, f = 500 mm was used to couple the Nd:YAG beam, and f = 300 mm was used to couple the higher M^2 value dye-laser beam.

The arrangement included a fiber-coupled signal-collection system that enables remote location of a custom-built spectrometer. The system employs a transmission-grating-based spectrometer with f/1.8 optics. The system also includes lenses, tapers, and a 10-m-long, bifurcated fiber-optic bundle used to collect and transmit two signals from the collection optics to the spectrometer. These components were located away from the engine to mitigate the effect of vibrations generated by the engine. The spectral resolution of the spectrometer was 0.02 nm, within a limited spectral range extending from 472 to 477 nm. The optical fiber bundle had a circular pattern, magnified by a custom taper. The output was linear and curved in an arc to counteract the curvature of the spectrometer optics.

Figure 3a is a photograph of the laser system installed in the PRF facility. The laser system is located ~5 m from the exhaust of the J85 engine, as shown in the upper right portion of Fig. 3a. Laser curtains were installed around the laser system for safety purposes. A hole cut in the curtain allowed the HCWGs to extend to the engine exhaust. The fiber-optic beam delivery system is shown in Fig. 3b.

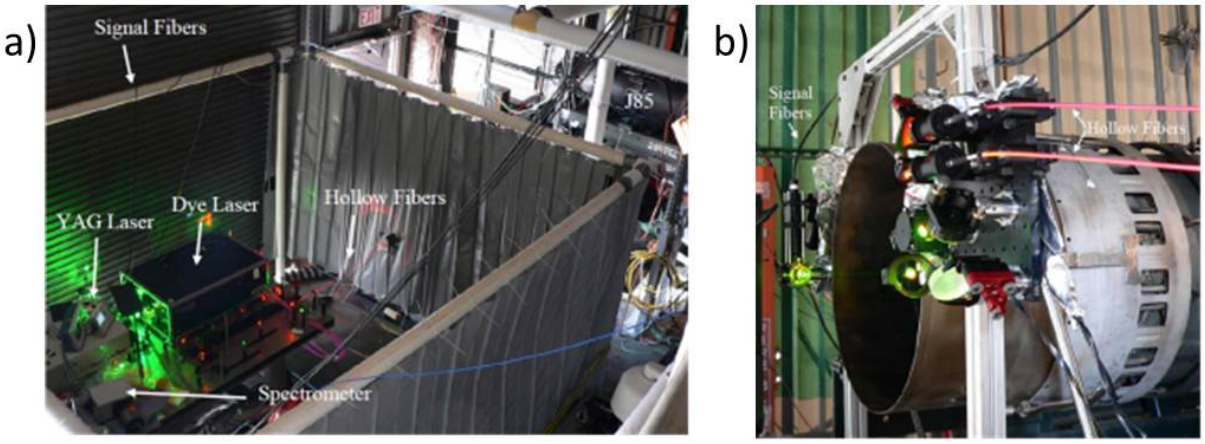

Figure 3. Photographs of the ns-HCWG CARS system during test demonstrations at the PRF facility. a) overhead photograph showing the laser system installation in relation to the J85 engine, b) photograph of the beam-delivery optics (foreground) and signal-collection optics (background) located downstream of the J85-engine nozzle exit plane.

A schematic diagram showing major components of the experimental setup is provided in Fig. 4. On the breadboard table shown on the left, laser beams were focused into the laser delivery HCWGs. These HCWGs delivered the beams to the beam-delivery optics mounted on a frame around the exhaust of the J85 engine. The CARS beam was collected through signal fibers and delivered to the spectrometer located on the same optical breadboard on which the laser beams were created.

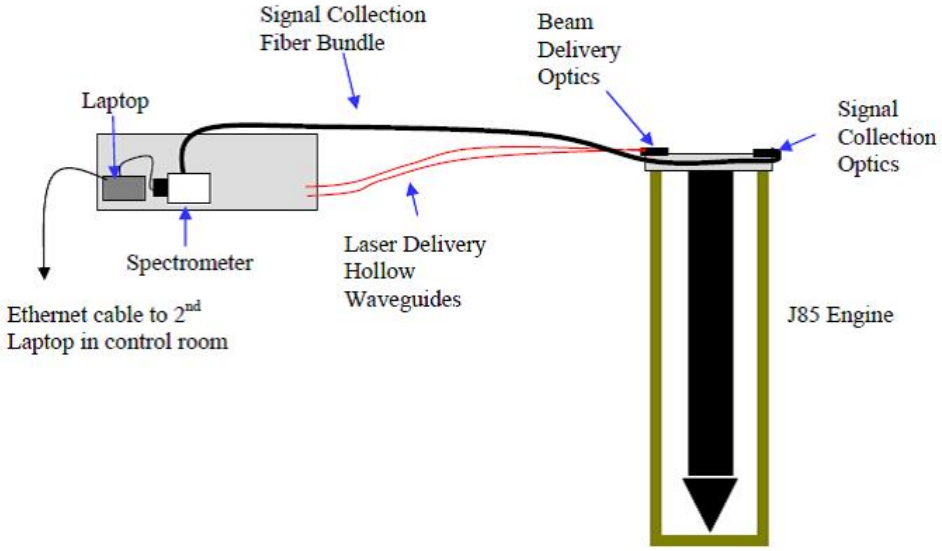

Figure 4. Schematic diagram of the ns-HCWG experimental setup at the PRF J85 site (not to scale).

Figure 5 includes a diagram of the beam delivery optics and signal-collection scheme surrounding the engine exit. The pump (532 nm) and Stokes (~607 nm) beams were collimated out from the HCWGs and then combined using a long-pass dichroic optic. For remote tweaking of the signal, a Newport motorized 2-in. mirror mount assembly was used to direct the beams through a focusing lens. The beams were focused to the center of the exhaust in a collinear phase-matching scheme. The CARS beam was filtered by reflecting off a long-pass dichroic, and then focused onto the signal-collection fiber-bundle. The signal fiber transported the CARS beam to the spectrometer.

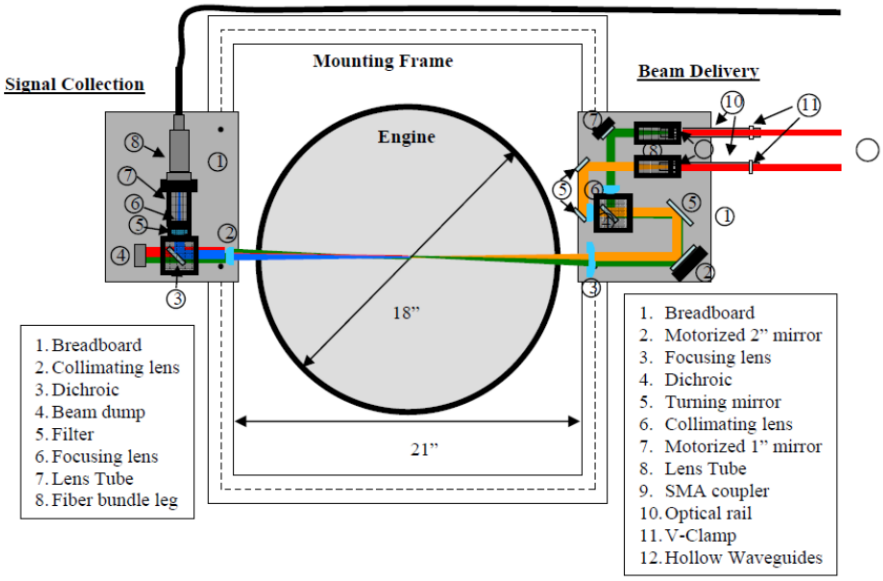

0

Figure 5. Schematic diagram of the experiment setup, aft looking forward.

CARS data were acquired at engine operating conditions ranging from Power Level Angle (PLA) values ranging from 15 deg (idle) to PLA 90 deg (full throttle, or full military, though not including afterburner). Figure 6 includes normalized average CARS spectra data acquired at various PLA engine operating conditions. An unidentified

spectral feature is noted near λ ~ 473.3 nm which increases in intensity as PLA increases. This feature is thought to be the result of the room lights background not being correctly subtracted.

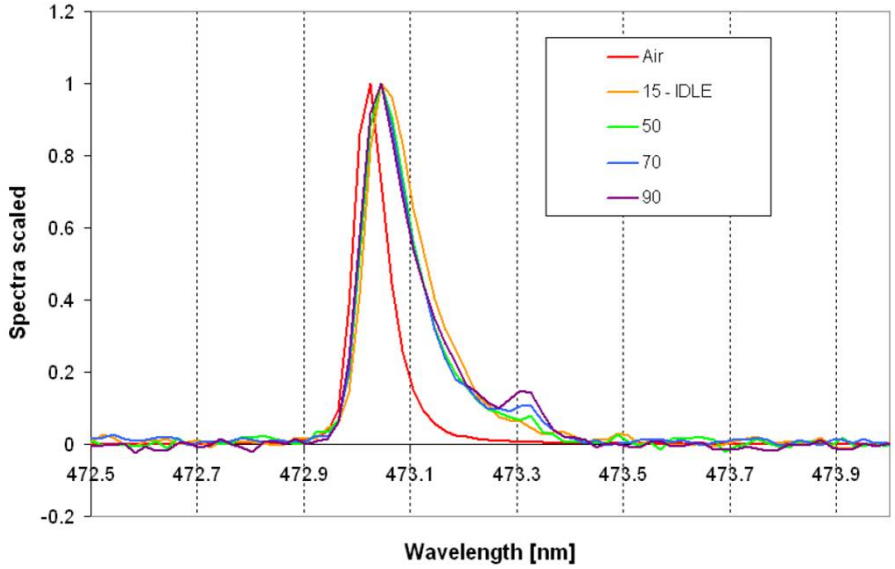

Figure 6. Normalized CARS spectral measurements acquired during J85 engine operations ranging from idle to military PLA conditions.

IV Application of the Transportable ps-CARS

Transportable ps-CARS System:

The transportable ps-CARS system consists of four basic subsystems: a 100-ps laser (Ekspla SL234), a custom-made, wavelength-tunable ps dye laser, two optical systems for direct-beam CARS in a BOXCARS configuration, and a fiber-coupled CARS in a collinear configuration. The entire system was built on two 4- × 3-ft breadboards to ensure transportability without misalignment of the system. To minimize effects of environmental factors on the laser system and the CARS optics, the ambient temperature, humidity, and vibration levels were controlled by enclosing the system within a special vibration and acoustic isolation structure and installing air conditioners and dehumidifiers within the structure. The transportable ps-CARS system is shown in Fig. 7.

Figure 7. Spectral Energies mobile ps-CARS system.

The ps laser (Ekspla, SL234) generates nearly Fourier-transform–limited, 532-nm laser pulses with output energies of ~106 mJ/pulse. The pulsewidth and the linewidth of this laser at 532 nm were ~100 ps and ~0.2 cm^{-1}, respectively. A fraction of the energy from the ps laser was used to pump a custom-built, modeless dye laser to generate broadband pulses at ~607 nm. The dye laser has a full-width at half-maximum (FWHM) bandwidth equal to ~135 cm^{-1}, a pulse duration equal to ~115 ps, and a maximum per-pulse energy equal to ~5 mJ. The 607-nm beam served as the Stokes beam. The 532-nm radiation was split into two beams to form the pump and probe beams for excitation of N_2 rotational-vibrational transitions. The per-pulse energies for the probe, pump, and Stokes beams were ~6.0 mJ, ~5.4 mJ, and ~1.2 mJ, respectively. These three beams were propagated over a 14-ft distance and then focused by a f = 300 mm spherical lens to the center of the J85 exhaust plane using a folded BOXCARS geometry. This geometry provides a cylindrical probe volume with dimensions equal to ~50 μm in diameter and ~2.0 mm in length. The N_2 CARS spectrum is dispersed by a 1.00-m spectrometer (Jobin Yvon Model SPEX 1000M) equipped with a 2,400-grove/mm grating. The spectra were recorded using a back-illuminated CCD camera (Andor Technologies Model DU 440BU). An overview of the experimental arrangement is provided in Fig. 8.

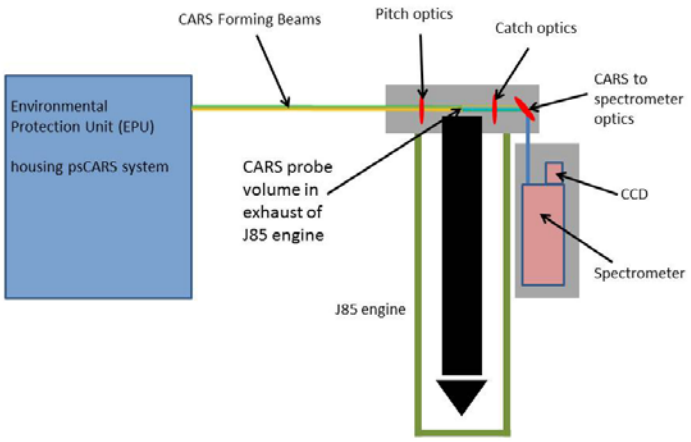

Figure 8. Schematic view of ps-CARS experimental setup at the PRF/J85 site.

Environmental Protection Unit (EPU):

Since the EKSPLA laser and the CARS optics are prone to misalignment and to degradation by humidity changes, mechanical and acoustic vibrations, temperature gradients, and dust, an Environmental Protection Unit (EPU) was built to house these components. The EPU was designed and fabricated to mitigate these issues. Figure 9 shows the transportable ps-CARS system installed inside the EPU. The EPU is a gable-style 10- × 12-ft engineered-wood storage shed which was modified to house a laser system located within the near vicinity of the J85 engine. The EPU floor material included two layers of 1-in. thick plywood. This floor is mounted on nine 6-in. diameter, 2-in.-wide, heavy-duty swivel casters having a thick plastic outer layer. The substantial weight of the EPU and installed laser system, ~3,500 lb, provides additional isolation from mechanical vibrations. During the course of the test campaign, there were no indications the EPU shifted due to the acoustic and mechanical vibrations experienced during J85 engine operations. The EPU was equipped with insulation, drywall, shingles, and an air-conditioning unit, heater, track lighting, dehumidifier, and air filter. The insulation and drywall of the EPU provide sufficient acoustic and vibration relief for the ps-CARS system, which allows stable CARS measurements to be acquired throughout J85 engine operations. A 3-in. hole was cut into the side of the EPU to allow the CARS forming beams to be transmitted from the EPU to the CARS focusing lens. The EPU was located roughly 14 ft from the engine.

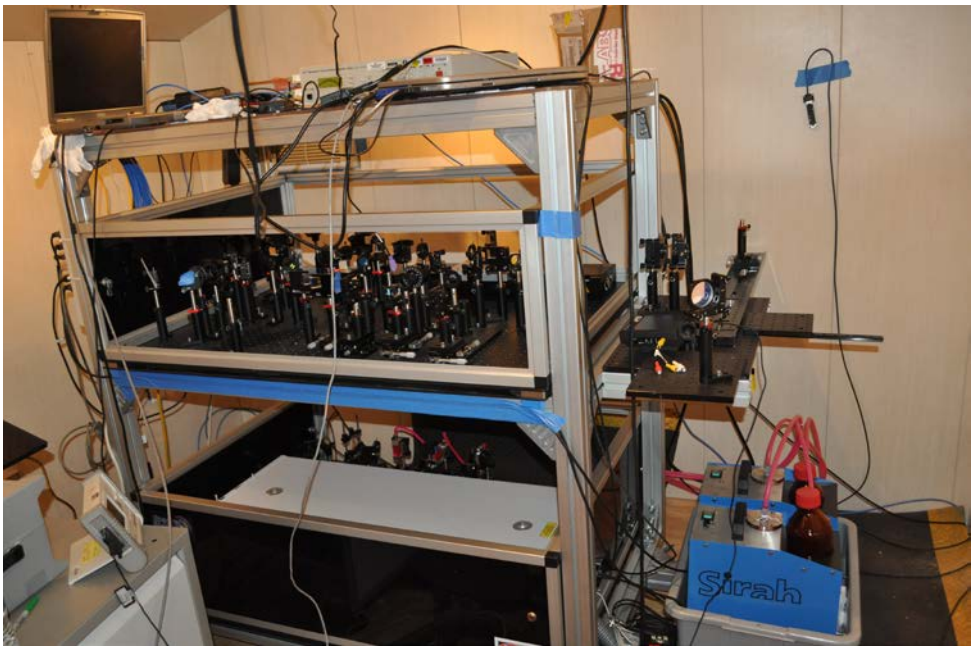

Figure 9. Photograph of the transportable ps-CARS system installed inside the EPU at the PRF/J85 site.

Detection System Protection:

Figure 9 displays the setup of the CARS signal-detection system installed in the PRF. The system was located ~1 m away from the J85 engine. Due to close proximity to the engine, the CARS signal-detection system experienced significant thermal heating during engine operations. Consequently, initially the camera was not adequately cooled, resulting in increased intrinsic noise levels. To mitigate this problem, a water-cooling device for the camera and a thermal acoustic blanket were installed. After the camera was stabilized, the signal detection system operated properly, as intended for subsequent engine tests (~ 4 to 5 hr). For vibrational CARS (VCARS), a narrow bandpass filter (Semrock, LD01-473/10-25.4) was used for signal collection. For rotational CARS (RCARS) measurements, a cross polarizer (w.r.t probe polarization) and a short-wave-length filter (Semrock, SPEN01) were used to reject the scattered light from the probe beam.

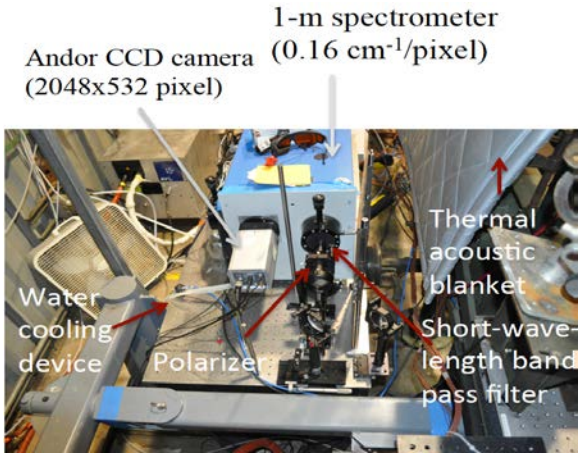

Figure 10. Detection system for CARS signal.

Picosecond Vibrational CARS Thermometry

The ps-VCARS was optimized at room air before the J85 engine testing began. The single-shot VCARS signal at room air reached ~300,000 counts with an SNR of ~10,000 (peak signal w.r.t noise level). The mean temperature and precision of the single-shot thermometry for the room-air case were within 1% and 2% of the set value, respectively. The data shown in Fig. 10 include a 20-shot-average nitrogen vibrational CARS spectrum taken in the J-85 exhaust. These data indicate the magnitude of the CARS signal is reduced by a factor of two, while the NRB signal is reduced by a factor of 25 at 100-ps delay. Point temperature measurements were performed at the center of the J85 engine exhaust flow. These data indicate the CARS signal decreased significantly during engine operations. It is speculated the decreased signal resulted from misalignment of the three CARS beams' attributable to vibrations experienced during engine operations. The misalignment resulted in degradation of the spatial overlapping volume of the three beams and displacement of the signal beam. To mitigate the beam-displacement issue, the spectrometer slit width was increased from 100 to 300 μm. However, this resulted in degrading the spectral resolution of the measurement. Figure 11 shows measured nitrogen spectra and associated temperature probability density functions (PDFs) derived from 25 spectra measurements during J85 PLA conditions equal to 15 (ground idle) and 90 (full military) deg. These spectra are shown as the square root of the signal intensity, which is proportional to the N_2 number density in the flow. To increase the SNR for the curve fitting process, each spectrum was averaged over 20 laser pulses. A comparison with the theoretical spectra obtained by the Sandia CARSFT code is shown in Fig. 11.[16] The temperature can be extracted from the CARS spectra by fitting the intensity and bandwidth of the primary N_2 band ($v = 0 \rightarrow v = 1$) . The data were acquired at a probe delay equal to 100 ps to remove the NRB contribution. The measured temperatures for engine settings at PLA 15 (ground-idle mode) and PLA 90 (full-military mode) agree with temperatures measured by diode-laser-based hyperspectral tomography included in Ref. 17. The CARSFT cannot fit the probe-pulse-delay spectrum perfectly. According to Ref. 18, the extracted temperature for the probe-delay spectra using CARSFT is expected to deviate at lower temperatures. Currently, analysis of the data utilizing a new fs/ps-CARS model based on Ref. 18 is in process.

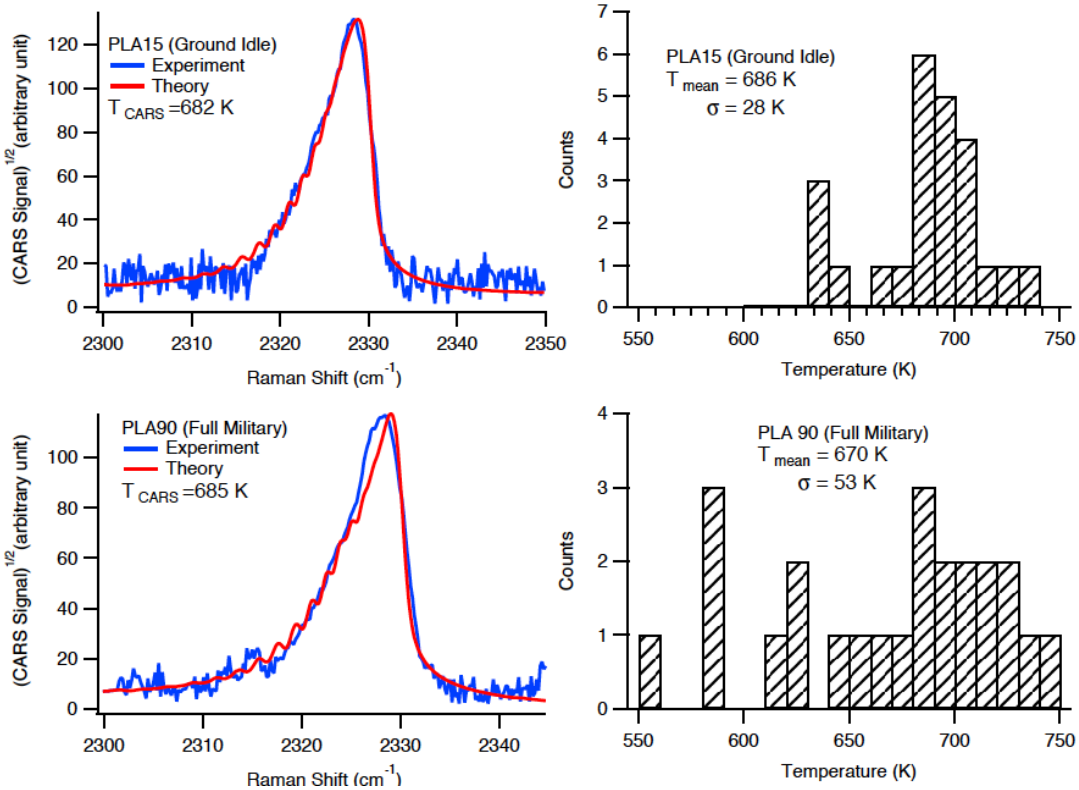

Figure 11. Plot (left): 20-shot-average nitrogen vibrational CARS spectrum taken in the exhaust of the J85 at PLA 15 and PLA90 compared to theory. Probability Density Function (right): Corresponding temperature PDFs for 25 consecutive 20-shot-average CARS spectra.

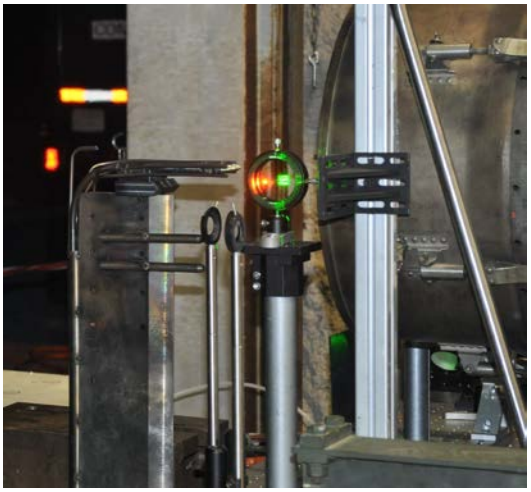

Figure 12 - Photo of two-beam ps-RCARS setup J85 engine exit plane.

Picosecond Rotational CARS thermometry

The ps-RCARS experimental apparatus is similar to the ps-VCARS setup, with the exception of a crossed two-beam geometry used in the VCARS setup, as shown in Fig. 12. This VCARS scheme is relatively easy to set up compared to the BOXCARS setup used by RCARS. In addition, because the pump and Stokes beams are automatically spatially overlapped, the technique is more robust in preventing vibration and turbulent beam-steering effects. This increases the suitability of VCARS for a diverse range of combustion conditions in practical engine environments. To mitigate misalignment resulting from engine vibration, the number of freestanding optics used near the engine, as compared to the ps-VCARS experiment, was minimized. As a result, single-shot ps-RCARS

thermometry was successfully demonstrated during J85 engine operations at military PLA level (15-90 deg). Figure 13 shows single-shot spectra measurements acquired at a J85 engine setting equal to PLA 60 deg. The spectrometer slit width was set at 100 μm. The measurements shown in Fig. 13 indicate the 100-ps delay effectively eliminates NRB interference. Room-temperature and high-temperature (engine setting of PLA 60) RCARS spectra for a 100-ps probe delay are shown in Fig. 14. The RCARS signals are attributed to N_2 and O_2. These measurements indicate higher rotational Q-branch lines for N_2 and O_2 appear at the high-temperature engine conditions. The preliminary measurements for single-shot RCARS room-air conditions are shown in Fig. 15. The intensity levels for each rotational line varied significantly for the steady room-air temperature measurements.

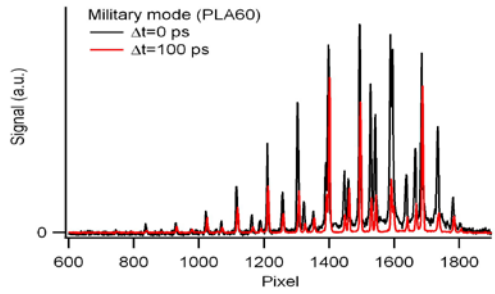

Figure 13. Single-shot spectra (corrected for dark counts) acquired during J85 engine operations at PLA 60 and a probe delay equal to 0 (back) and 100 ps (red).

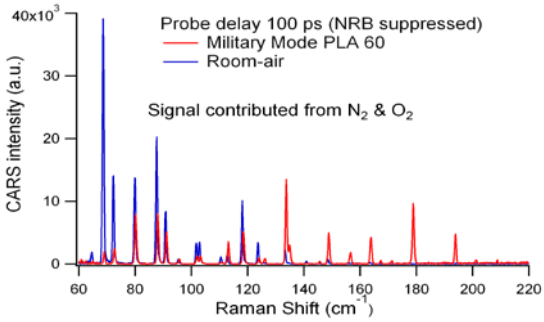

Figure 14. Single-shot spectra for room air conditions (blue) and the J85 engine operations at PLA 60 g (red).

Since the line intensities of the Q-branch transitions of N_2 and O_2 were employed to extract the temperature using Boltzmann plots, the fluctuating line intensity for the single-shot room-air RCARS data will result in inaccurate single-shot thermometry. Figure 15b shows that the temperature can be determined accurately by 100-laser-shot average RCARS data. It was initially speculated that the fluctuation-of-line-intensities could result from the mode-structure, particularly the phase portion of the fluctuations in the ps-pulsed dye laser. Analyses of the single-shot, high-temperature RCARS data from the engine measurements are needed to further investigate dye-laser phase-instability.

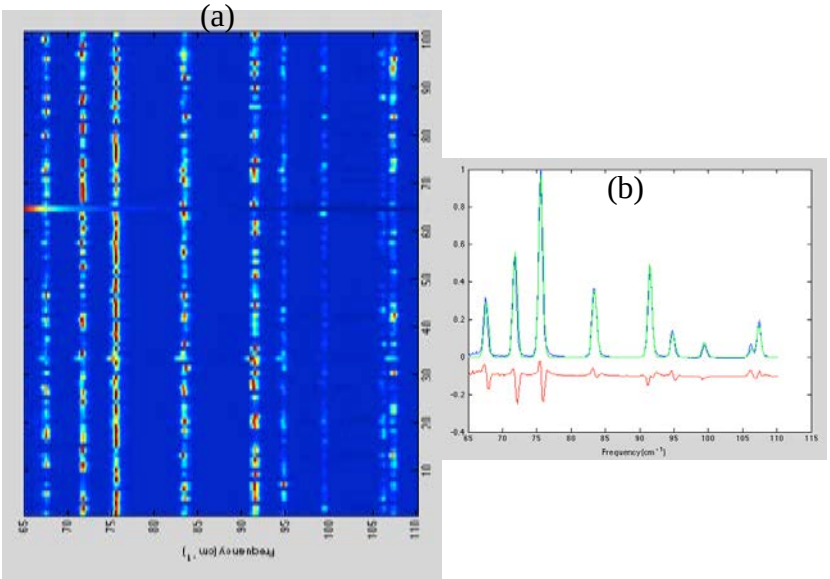

Figure 15. (a) Distribution of 100 single-shot RCARS spectra. (b) Fitted experimental 100-shot-average spectrum acquired at room-air condition and delay equal to 100 ps.

V Summary

Nanosecond-laser-based fiber-coupled VCARS, ps-laser-based direct-beam VCARS, and RCARS were successfully demonstrated in the PRF test bed to acquire spectral measurements and derive temperatures in the exhaust of a J85 turbojet engine. The demonstrations required improvements and modifications to accommodate CARS measurements inside engine test facilities. These improvements include using HCWGs and free-space beam-guiding for the ns-CARS and ps-CARS system using a folded BOXCARS and crossed two-beam geometry. The ps-CARS system used a probe delay technique to suppress the NBR portion of the signal. A transportable, specially designed EPU was shown to reduce the risks associated with use of the ps-CARS system in harsh test cell environments located within close vicinity of the turbine engine operations. Preliminary analysis to derive temperatures using CARS spectra measurements were shown using three techniques. This work shows significant promise for utilizing fiber-coupled ns- and ps-CARS spectroscopy to acquire beneficial diagnostic measurements in turbine-engine ground test facilities.

Acknowledgments

This work was funded in large part by the SBIR program at AEDC. The ns-CARS system is an SBIR product delivered to AEDC by OKSI. The ps-CARS system is an SBIR product delivered to AEDC by Spectral Energies. This work was conducted by the Aerospace Testing Alliance (ATA), the AEDC operating contractor, and jointly funded by the US Air Force Research Laboratory under Contract No. FA8650-10-C-2008 and the US Air Force Arnold Engineering and Development Complex (AEDC) under Contract Nos. FA9101-08-0015, FA9101-09-C-0031. The technical support from the AEDC/UTSI PRF test team, Opto-Knowledge Systems Inc. (OKSI), and Spectral Energies is gratefully acknowledged. This manuscript is cleared for public release by the AEDC STINFO Officer and AEDC Public Affairs.

References

[1]Eckbreth, A. C., *Laser Diagnostics for Combustion Temperature and Species*, 2nd ed., Gordon and Breach, Netherlands, 1996.

[2]Roy, S., Gord, J. R., and Patnaik, A. K. "Recent Advances in Coherent Anti-Stokes Raman Scattering Spectroscopy: Fundamental Developments and Applications in Reacting Flows," *Prog. Energy Combust. Sci.* Vol. 36, p. 280, 2010.

[3]Meyer, T. R., Roy, S., and Gord, J. R. "Improving Signal-to-Interference Ratio in Rich Hydrocarbon-Air Flames Using Picosecond Coherent Anti-Stokes Raman Scattering," *Appl. Spectrosc.* Vol. 61, p. 1135, 2007.

[4]Seeger, T., Kiefer, J., Leipertz, A., Patterson, B. D., Kliewer, C. J., and Settersten, T. B., "Picosecond Time-Resolved Pure Rotational Coherent Anti-Stokes Raman Spectroscopy for N_2 Thermometry," *Opt. Lett.* Vol. 34, p. 3755, 2009.

[5]Kulatilaka, W. D., Hsu, P. S., Stauffer, H. U., Gord, J. R., and Roy, S., "Direct Measurement of Rotationally Resolved H-2 Q-Branch Raman Coherence Lifetimes Using Time-Resolved Picosecond Coherent Anti-Stokes Raman Scattering," *Appl. Phys. Lett.* Vol. 97, p.081112, 2010.

[6]Miller, J. D., Roy, S., Gord, J. R. and Meyer, T. R., "Communication: Time-Domain Measurement of High-Pressure N_2 and O_2 Self-Broadened Linewidths Using Hybrid Femtosecond/Picosecond Coherent Anti-Stokes Raman Scattering," *J. Chem. Phys.* Vol. 135, p. 201104, 2011.

[7]Roy, S., Hsu, P. S., Jiang, N., Gord, J. R., Kulatilaka, W. D., Stauffer, H. U., and Gord, J.R. "Direct Measurements of Collisionally Broadened Raman Linewidths of CO_2 S-Branch Transitions," *J. Chem. Phys.* Vol.138, p. 024201, 2013.

[8]Hsu, P. S., Jiang, N., Stauffer, H. U., Gord, J. R., and Roy, S., "Direct Measurements of Collisional Raman Line Broadening in the S-Branch Transitions of Acetylene (C_2H_2)," *J. Chem. Phys.* Vol. 139, p. 154201, 2013.

[9]Roy, S., Kulatilaka, W. D., Richardson, D. R., Lucht, R. P., and Gord, J. R., "Gas-Phase Single-Shot Thermometry at 1 kHz Using fs-CARS Spectroscopy," *Opt. Lett.* Vol. 34, p. 3857, 2009.

[10]Miller, J. D., Dedic, C. E., Roy, S., Gord, J. R., and Meyer, T. R., "Interference-Free Gas-Phase Thermometry at Elevated Pressure Using Hybrid Femtosecond/Picosecond Rotational Coherent Anti-Stokes Raman Scattering," *Opt. Express* Vol. 20, p. 5003, 2012.

[11]Vereschagin, K. A., Smirnov, V. V., Stelmakh, O. M., Fabelinsky, V. I., Sabelnikov, V. A., Ivanov, V. V., Clauss, W., Oschwald, M., "Temperature Measurements by Coherent Anti-Stokes Raman Spectroscopy in Hydrogen-Fueled Scramjet Combustor," *Aerosp. Sci. Technol*. Vol. 5, pp. 347-355, 2001.

[12]Magnotti, G., Cutler, A. D., and Danehy, P. M., "Beam Shaping for CARS Measurements in Turbulent Environments," *Appl. Opt.* Vol. 51, p. 4730, 2012.

[13]Kriesel, J. M., Garman, J. D., Hagglund, G. M., Gat, N., Papac, M. J., Dunn-Rankin, D., and Danczyk, S.A.," Compact and

Rugged Coherent Anti-Stokes Raman Spectroscopy (CARS) System for Measurements of Temperature in Rocket Test Stands and Other Harsh Operation Environments," *Proceedings of JANNAF 42nd Combustion Subcommittee Meeting*, Boston, MA, May 2008.

[14]Hsu, P. S., Patnaik, A. K., Gord, J. R., Meyer, T. R., Kulatilaka, W. D., and Roy, S., "Investigation of Optical Fibers for Coherent Anti-Stokes Raman Scattering (CARS) Spectroscopy in Reacting Flows," *Exp. Fluids* Vol. 49, p. 969, 2010.

[15]Hsu, P. S., Kulatilaka, W. D., Gord, J. R., and Roy, S., "Single-Shot Thermometry Using Fiber-Based Picosecond Coherent Anti-Stokes Raman Scattering (CARS) Spectroscopy" *J. Raman Spectrosc*. Vol. 44, p. 1330, 2013.

[16]Kriesel, J. M., Gat, N., and Plemmons, D., "Fiber Optics for Remote Delivery of High Power Pulsed Laser Beams," AIAA Paper 2010-1305 (2010).

[17]Savage, K., Beitel, G., Hiers, R., and Schulz, R., "Test Capabilities in the AEDC/UTSI J85 Turbojet Test Stand," AIAA Paper 2007-1658, 2007.

[16]Palmer, R. E., Report SAND89-8206, Sandia National Laboratories, Livermore, CA, 1989.

[17]Ma., L., Li, X., Sanders, S. T., Caswell, A.W., Roy, S., Plemmons, D. H., and Gord, J. R., "50-kHz-rate 2D Imaging of Temperature and H_2O Concentration at the Exhaust Plane of a J85 Engine Using Hyperspectral Tomography," *Opt. Express* Vol. 21, 1152, 2013.

[18]Stauffer, H. U., Miller, J. D., Slipchenko, M. N., Meyer T. R., Prince, B. D., Roy, S., and Gord, J. R., "Time-and Frequency-Dependent Model of Time-Resolved Coherent Anti-Stokes Raman Scattering (CARS) with a Picosecond-Duration Probe Pulse," *J. Chem. Phys.* Vol. 140, p. 024316, 2014.